Novel salivary antihemostatic activities of long-form D7 proteins from the malaria vector *Anopheles gambiae* facilitate hematophagy

Leticia Barion Smith[‡]🆔, **Emma Duge**[‡]🆔, **Paola Carolina Valenzuela-León**🆔, **Steven Brooks**🆔, **Ines Martin-Martin**🆔, **Hans Ackerman**🆔, and **Eric Calvo**[*]🆔

From the Laboratory of Malaria and Vector Research, National Institutes of Allergy and Infectious Diseases, National Institutes of Health, Bethesda, Maryland, USA

Edited by F. Peter Guengerich

To successfully feed on blood, hematophagous arthropods must combat the host's natural hemostatic and inflammatory responses. Salivary proteins of blood-feeding insects such as mosquitoes contain compounds that inhibit these common host defenses against blood loss, including vasoconstriction, platelet aggregation, blood clotting, pain, and itching. The D7 proteins are some of the most abundantly expressed proteins in female mosquito salivary glands and have been implicated in inhibiting host hemostatic and inflammatory responses. *Anopheles gambiae*, the primary vector of malaria, expresses three D7 long-form and five D7 short-form proteins. Previous studies have characterized the AngaD7 short-forms, but the D7 long-form proteins have not yet been characterized in detail. Here, we characterized the *A. gambiae* D7 long-forms by first determining their binding kinetics to hemostatic agonists such as leukotrienes and serotonin, which are potent activators of vasoconstriction, edema formation, and postcapillary venule leakage, followed by *ex vivo* functional assays. We found that AngaD7L1 binds leukotriene C4 and thromboxane A2 analog U-46619; AngaD7L2 weakly binds leukotrienes B4 and D4; and AngaD7L3 binds serotonin. Subsequent functional assays confirmed AngaD7L1 inhibits U-46619-induced platelet aggregation and vasoconstriction, and AngaD7L3 inhibits serotonin-induced platelet aggregation and vasoconstriction. It is therefore possible that AngaD7L proteins counteract host hemostasis by scavenging these mediators. Finally, we demonstrate that AngaD7L2 had a dose-dependent anticoagulant effect *via* the intrinsic coagulation pathway by interacting with factors XII, XIIa, and XI. The uncovering of these interactions in the present study will be essential for comprehensive understanding of the vector-host biochemical interface.

Anopheles gambiae is the major African vector of the malaria *Plasmodium* parasites that afflict more than 200 million people and causes over 400,000 deaths each year worldwide (1). Transmission of *Plasmodium* sporozoites to the host occurs during blood feeding, for which mosquito saliva plays a critical role.

When a female mosquito takes a blood meal, the resulting tissue injury exposes collagen and other matrix molecules which activate the host's hemostasis response. During hemostasis, the host's blood vessels constrict, platelets aggregate, and blood clotting occurs to minimize blood loss and disrupt the ability of the mosquito to blood feed. Many blood-feeding arthropods have independently evolved pharmacologically active salivary compounds that inhibit host hemostatic and inflammatory responses and enable them to successfully blood feed (2).

Many of the hemostasis processes that mediate a variety of early responses to wounding are regulated, at least to some extent, by biogenic amines and eicosanoids. Biogenic amines that regulate blood clotting, vasoconstriction, and inflammation are released by platelets, mast cells, and sympathetic neurons with the onset of feeding (3). Eicosanoids, secreted by mast cells, affect swelling, itching, and pain at the bite site (4). Inhibiting these processes is important for avoiding host defensive behaviors that may interrupt feeding. Many salivary proteins neutralize the small-molecule effectors of hemostasis and inflammation by rapidly binding them with abundant proteins having high-affinity ligand-binding sites (3, 5, 6). The D7 family of proteins from mosquitoes, among others, has been found to act in this manner (3, 7, 8). An evolutionary arms race between arthropod blood feeders and their vertebrate hosts has resulted in a plethora of diverse salivary proteins, many arising from gene duplication events, needed to bind the widely varying small-molecule effectors in the host (9).

The D7 protein family is specifically expressed in the salivary glands of adult *Diptera* and are some of the most abundantly expressed proteins in the salivary glands of female mosquitoes (7, 10). The D7s are a multi-gene family with two subfamilies in mosquitoes: the short-forms range from 15 to 20 kDa and have a single binding domain, and the long-forms are 27 to 30 kDa and possess both C-terminal– and N-terminal–binding domains (11–15). The C-terminal–binding pocket is negatively charged and has been observed to bind

biogenic amines (3). The N-terminal–binding pocket is distinct in sequence and structure; it is positively charged and scavenges cysteinyl leukotrienes (CysLTs) and other biolipids (14).

The D7 proteins are among the most abundant of the potent antihemostatic salivary proteins from the female *A. gambiae* (3, 13). *A. gambiae* has five short-form and three long-form D7 proteins (13). The short-forms D7r1-4 are homologous to the *Aedes* D7 C-terminal–binding domain and bind biogenic amines. D7r5 has low expression yields, no observable binding activity, and is proposed to be a pseudogene (3). Although the *A. gambiae* short-forms have been characterized extensively, the functionalities of the long-form proteins have not been investigated.

In this study, we investigate the ligand-binding specificity and physiological function *ex vivo* of the three *A. gambiae* long-form salivary proteins: AngaD7L1, AngaD7L2, and AngaD7L3. Protein sequence alignments suggested AngaD7L1 and AngaD7L2 involvement in lipid binding and AngaD7L3-binding serotonin, which were confirmed by isothermal titration calorimetry (ITC). We found that AngaD7L1 binds thromboxane A2 analog, U-46619, and leukotriene C_4 (LTC$_4$) and reduces U-46619-induced platelet aggregation and vasoconstriction. AngaD7L2 weakly binds the leukotriene B_4 (LTB$_4$) and D_4 (LTD$_4$) and induces anticoagulation *via* the intrinsic coagulation pathway by reducing the generation of factor XIIa (FXIIa) and factor XIa in plasma. Finally, AngaD7L3 is the first characterized anopheline D7 long-form protein to bind a biogenic amine, serotonin, resulting in diminished platelet aggregation and vasoconstriction.

Results

Sequence alignment and initial characterization

The AngaD7L1 and AngaD7L2 amino acid sequences are 63% and 76% similar, respectively, to that of the *Anopheles stephensi* D7L1 protein, a protein previously shown to bind CysLTs and U-46619 (16). The specific residues involved in lipid binding in the N-terminal–binding pocket were found to be highly conserved in AngaD7L1 (9 of 11) and entirely conserved in AngaD7L2 (11 of 11) (Fig. S1). Similarly, AngaD7L3 exhibits 100% conservation (9 of 9) of C-terminal residues involved in the binding of serotonin as revealed by molecular modeling of AeD7L1 and the *A. gambiae* D7 short-forms (3, 8, 17). Notably, the position of the highly conserved biogenic amine-binding residue in AeD7L1 (His 189) and the *A. gambiae* short-forms D7r1-4 is conserved in AngaD7L3

(His 228). This residue is responsible for the binding of D7 proteins with serotonin and catecholamines through hydrogen bonding through their phenolic hydroxyl groups (14).

Recombinant protein expression and purification

Recombinant AngaD7L1, AngaD7L2, and AngaD7L3 were expressed in human embryonic kidney cells and purified by ion-exchange and size-exclusion chromatography as described in Experimental procedures (Fig. S2, *A–C*). The identity of purified recombinant proteins was confirmed by N-terminal sequencing and visualized as a single band by Coomassie-staining gel electrophoresis (Fig. S2*D* and Table S1).

ITC reveals novel binding activity of A. gambiae D7 long-form proteins

We screened each of the three AngaD7 long-form proteins against five biogenic amines (serotonin, histamine, epinephrine, norepinephrine, and tryptamine) and five lipids (leukotrienes B4, C4, D4, and E4, U-46619) involved in the hemostatic and inflammatory responses and previously observed to bind D7L proteins in other mosquito species using PEAQ-ITC to determine the dissociation constant (K$_D$) of each protein ligand combination and provide insight into their potential roles in blood feeding. The scavenging mechanism of action requires a high concentration of salivary protein at the bite site. As D7 proteins bind their ligands in a 1:1 stoichiometric ratio, they must be in equimolar concentrations with the mediators, which range from 1 to 10 μM for histamine and serotonin (18). This may explain why D7 salivary proteins are one of the most abundant components of the salivary glands. In all cases, stoichiometries suggested a single ligand-binding site for all ligands tested (N $\sim$ 6 × 10^{-1}–1 × 10^0) (Table 1, Figs. 1, and S3–S5). AngaD7L1 was observed to bind U-46619 (K$_D$ = 4 × 10^2 ± 2 × 10^2 nM) and LTC$_4$ (K$_D$ = 2 × 10^3 ± 2 × 10^3 nM). AngaD7L2 binds LTB$_4$ (K$_D$ = 8 × 10^2 ± 1 × 10^3 nM) and LTD$_4$ (K$_D$ = 1 × 10^3 ± 1 × 10^3 nM). AngaD7L3 binds serotonin (K$_D$ = 2 × 10^1 ± 4 × 10^0 nM), a novel activity for a member of the anopheline D7 long-form family. Given the K$_D$ values between ligands and their receptors are in the nM range (19), AngaD7Ls would be a good competitor for scavenging these molecules at the bite site.

### A. gambiae D7L proteins inhibit platelet aggregation in vitro

AngaD7L1 binds the platelet aggregation mediator thromboxane A2 (TxA2) analog U-46619 (Fig. 1) and, therefore, we hypothesized AngaD7L1 functions as a platelet aggregation

Table 1
Thermodynamic parameters of *Anopheles gambiae* D7 long-form proteins with biogenic amine and eicosanoid ligands measured by PEAQ-ITC

Protein	Ligand	K$_D$ ± SD (nM)	ΔH ± SD (cal/mol)	−TΔS ± SD (cal/mol/deg)	Stoichiometry± SD
AngaD7L1	LTC$_4$	2 × 10^3 ± 2 × 10^3	−3 × 10^1 ± 3 × 10^1	2 × 10^1 ± 4 × 10^1	9 × 10^{-1} ± 4 × 10^{-1}
	U-46619	4 × 10^2 ± 2 × 10^2	−9 × 10^0 ± 2 × 10^0	5 × 10^0 ± 1 × 10^0	7 × 10^{-1} ± 2 × 10^{-1}
AngaD7L2	LTB$_4$	8 × 10^2 ± 1 × 10^3	−3 × 10^1 ± 5 × 10^{-1}	1 × 10^1 ± 5 × 10^1	6 × 10^{-1} ± 3 × 10^{-1}
	LTD$_4$	1 × 10^3 ± 1 × 10^3	−4 × 10^1 ± 3 × 10^1	3 × 10^1 ± 3 × 10^1	1 × 10^0 ± 2 × 10^0
AngaD7L3	Serotonin	2 × 10^1 ± 4 × 10^0	−6 × 10^0 ± 9 × 10^{-1}	−5 × 10^0 ± 9 × 10^{-1}	1 × 10^0 ± 4 × 10^{-2}

A minimum of three replicates were performed per protein–ligand interaction.
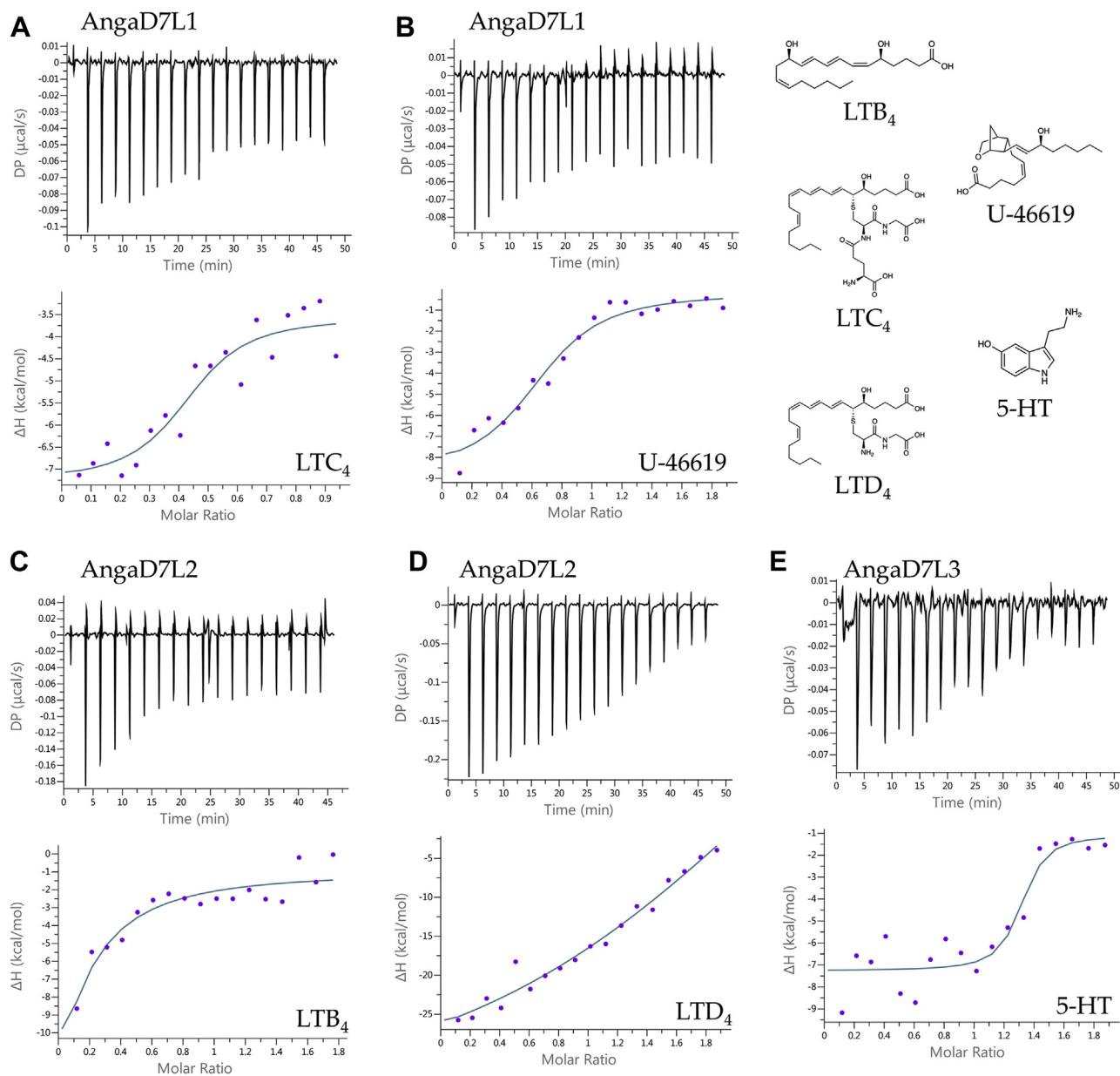
Figure 1. PEAQ-Isothermal titration calorimetry with AngaD7 long-form recombinant proteins reveals binding with biogenic amines and lipids involved in hemostasis. PEAQ-ITC trials conducted using 1:10 protein to ligand concentrations in TBS. AngaD7L1 binds (*A*) LTC4 and (*B*) U-46619; AngaD7L2 binds (*C*) LTB4 and (*D*) LTD4; and AngaD7L3 binds (*E*) serotonin (5-HT). Titration curves are representative of at least three measurements. ITC, isothermal titration calorimetry.

inhibitor. Platelet aggregation occurs very quickly upon tissue injury as a mechanism to prevent further blood loss. Exposure to collagen, from the subendothelial matrix, or thrombin initiates the formation of a platelet monolayer and the subsequent adhesion of activated platelets, ultimately forming a platelet plug (9, 20, 21). At low collagen concentrations, TxA2 plays an important role in the extension and amplification of platelet aggregation, but at high concentrations, collagen can induce platelet aggregation independently of TxA2 by acting as a strong agonist of the GPVI receptor on the platelet surface (20). While D7 proteins do not bind collagen directly, they sequester molecules such as TxA2 that amplify the platelet aggregation process and thus reduce the effect. Hence, we

expect to see platelet aggregation inhibition at low collagen concentrations but not at high concentration. We used a low collagen concentration of 1 μg/ml for most assays. At a low protein concentration (0.3 μM), AngaD7L1 did not inhibit platelet aggregation (Fig. 2). At 1 μM, AngaD7L1 had a slight effect on inhibiting platelet aggregation with the low collagen concentration (1 μg/ml) (Fig. 2) but no effect with high collagen concentration (10 μg/ml). At 3 μM, AngaD7L1 reduced platelet aggregation at the 1 μg/ml concentration of collagen. When platelet aggregation was initiated with U-46619, AngaD7L1 had a dose-dependent inhibitory effect on platelet aggregation. At a high dose of U-46619 (0.7 μM), 0.3 μM AngaD7L1 did not have any effect in inhibiting
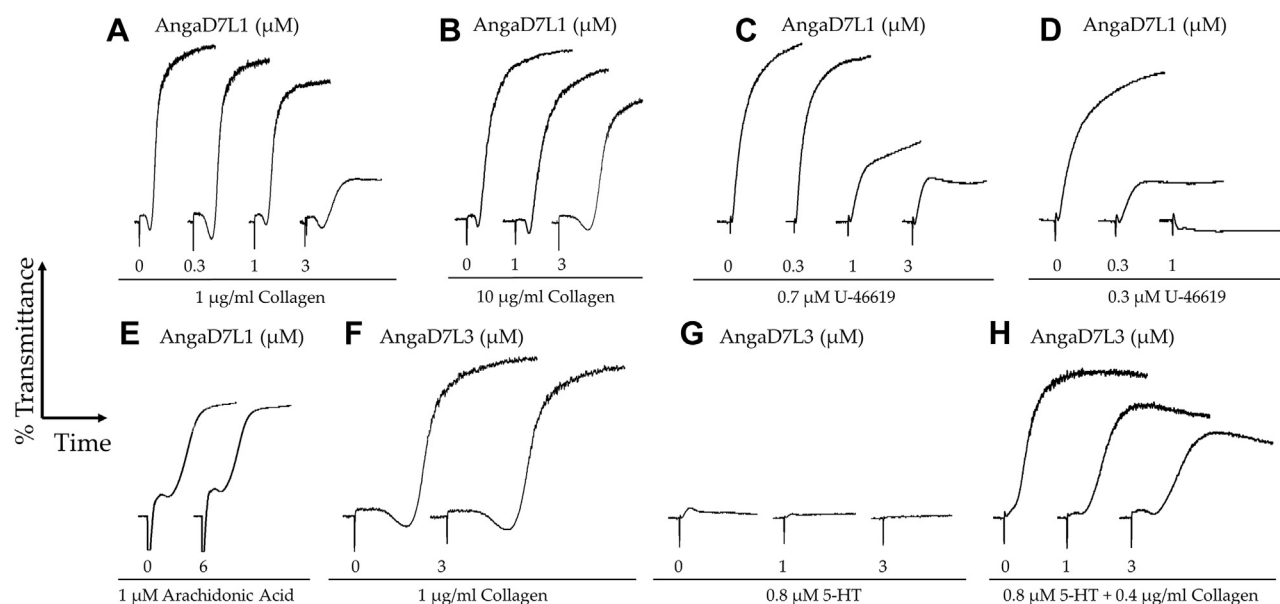
Figure 2. Effects of AngaD7 long-form proteins on platelet aggregation. Platelet-rich plasma (PRP) was incubated with varying concentrations of each recombinant protein independently before the addition of platelet agonists. AngaD7L1 at various concentrations with agonist (*A*) 1 μg/ml collagen, (*B*) 10 μg/ml collagen, (*C*) 0.7 μM U-46619, (*D*) 0.3 μM U-46619, (*E*) 1 μM arachidonic acid, and AngaD7L3 at various concentrations with agonists (*F*) 1 μg/ml collagen, (*G*) 0.8 μM 5-HT, and (*H*) 0.8 μM 5-HT + 0.4 μg/ml collagen. Protein concentrations are indicated in μM under each curve. Individual curves represent the change in % transmittance over time.

aggregation. However, when a lower U-46619 dose (0.3 μM) was used, the lower concentration of AngaDL71 reduced platelet aggregation. Similarly, at a concentration of 1 μM of AngaD7L1, platelet aggregation was inhibited at both high and low U-46619 concentrations, but the effect was strongest at the lower concentration of U-46619. Finally, at a high concentration of protein (3 μM), AngaD7L1 inhibited platelet aggregation at the high concentration of U-46619. AngaD7L1 had no effect on the TxA2 precursor, arachidonic acid, at any concentration.

AngaD7L3 tightly binds serotonin (Table 1 and Fig. 1), which is a platelet aggregation mediator and potentiator of platelet agonists such as ADP and collagen. We therefore hypothesized that AngaD7L3 also functions as a platelet aggregation inhibitor. At the highest protein concentration (3 μM) and low collagen concentration (1 μg/ml), AngaD7L3 had no collagen-induced effect on platelet aggregation (Fig. 2). However, at the 3 μM concentration, AngaD7L3 did reduce platelet aggregation when induced by serotonin alone (but not at 1 μM of AngaD7L3). Serotonin alone is not a potent agonist, and while it can induce platelet shape change, the platelets eventually disaggregate (22). We therefore combined serotonin and collagen to produce a full aggregation response. AngaD7L3 had a dose-dependent inhibitory effect on platelet aggregation when incubated with serotonin + collagen, inhibiting aggregation the strongest at the high concentration of 3 μM of AngaD7L3 (Fig. 2).

A. gambiae *salivary D7L1 and D7L3 proteins are vasodilators*

AngaD7L1 binds U-46619, an analog of the potent vaso-constrictor thromboxane A2 (TxA2); similarly, AngaD7L3 binds serotonin which is also a potent vasoconstrictive agonist (Fig. 1). We therefore hypothesized that the AngaD7L1 and

AngaD7L3 salivary proteins would act to abrogate vasoconstriction to U-46619 and serotonin, respectively, in *ex vivo* murine resistance arteries. To better understand the effect of these salivary proteins on vasodilation, we used equimolar concentrations of agonists and salivary proteins, in keeping with the 1:1 stoichiometry determined in our ITC studies. In third-order mesenteric arteries (n = 6, three male and three female), U-46619 induced a rapid, dose-dependent vasoconstriction (Fig. 3, *A* and *C*) with logIC50 = −8.2 (Table 2). Following incubation with AngaD7L1 (10 μM), the vasoconstrictive response to U-46619 was significantly inhibited, shifting the logIC50 to −6.4, indicating ~70-fold reduction in effective constrictive potency of U-46619 in the presence of AngaD7L1. After washout of AngaD7L1, the vasoconstrictive potency of U-46619 was restored (logIC50 = −8.2). No effect of mouse sex was observed on vasoconstrictive potency of U-46619 at baseline or after addition of AngaD7L1. In a separate set of third-order mesenteric arteries (n = 7, three female and four male), serotonin induced potent dose-dependent vasoconstriction (Fig. 3, *B* and *D*) with logIC50 = −7.0 (Table 2). Following incubation with AngaD7L3 (1 μM), the vasoconstrictive response to serotonin was significantly inhibited, shifting the logIC50 = −5.6, indicating ~25-fold reduction in effective constrictive potency of serotonin in the presence of 1 μM AngaD7L3. After washout of AngaD7L3, the vasoconstrictive potency of serotonin was restored (logIC50 = −6.9). No effect of mouse sex was observed on vasoconstrictive potency of 5-Hydroxytryptamine (5-HT) at baseline or after addition of AngaD7L3.

AngaD7L2 displays anticoagulant activity in normal plasma

The three recombinant proteins were each tested for anti-coagulant properties by performing plasma recalcification
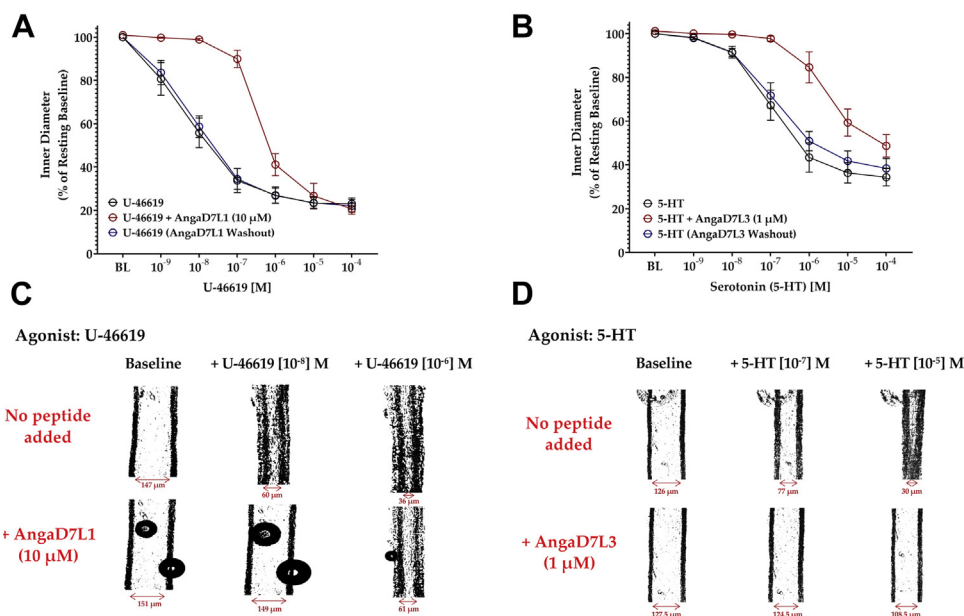
Figure 3. AngaD7L1 inhibits vasoconstriction to U-46619, and AngaD7L3 inhibits constriction to serotonin, in isolated murine resistance arteries. Third-order mesenteric arteries from C57Bl/6J mice were cannulated in an *ex vivo* pressure myograph system to measure vasoconstriction in response to the agonists (*A*) U-46619 (n = 6) and (*B*) serotonin (5-HT, n = 7) (*black lines*). After dose-response vasoconstriction was measured to each agonist, arteries were incubated with AngaD7L1 (10 μM) and constricted again with U-46619 or AngaD7L3 (1 μM) and constricted again with 5-HT (*red lines*). The salivary gland peptides were then washed off, and a final constriction curve to either U-46619 or 5-HT was performed (*blue lines*). AngaD7L1 (10 μM) significantly inhibited the sensitivity to constriction with U-46619, shifting the logIC50 from −8.2 to −6.4, and AngaD7L3 (1 μM) significantly inhibited the sensitivity to constriction with serotonin, shifting the logIC50 from −7.0 to −5.6 (Table 2). *C* and *D*, representative artery images of the vasoconstrictive responses to U-46619 or 5-HT in the absence or presence of peptide. *C*, images of an area of a single artery taken at baseline and then following constriction to [10-8]M U-46619 and [10-6]M U-46619, with and without the AngaD7L1 peptide. *D*, images of an area of a single artery taken at baseline and then following constriction to [10-7] M 5-HT and [10-5]M 5-HT, with and without the AngaD7L3 peptide. The inner diameter of the artery for each response is displayed below (μm).

assays. Samples containing AngaD7L1 and AngaD7L3 coagulated at a rate similar to that of the negative control containing Hepes buffer alone (Fig. 4*A*). However, AngaD7L2 exhibited a dose-dependent anticoagulant response (Fig. 4*A*). This is a novel activity never reported in a member of any long-form of D7 proteins. The samples with the highest concentration of AngaD7L2 (final concentration 5 μM) were entirely unable to coagulate and comparable to the response observed with the potent anticoagulant positive control, Alboserpin (3 μM), an FXa-directed anticoagulant from the saliva of *Aedes albopictus* (23) (5 μM, $p < 0.0001^{****}$; 2.5 μM, $p = 0.0036^{**}$).

Prothrombin and activated partial thromboplastin clotting times show that AngaD7L2 targets the intrinsic pathway of coagulation

To determine which clotting pathway AngaD7L2 is involved in, we performed prothrombin (PT) and activated partial

Table 2
Vasodilatory parameters of AngaD7L1 and AngaD7L3 by murine mesenteric artery myography

| Treatment	LogIC$_{50}$	SEM	*p*-value
U-46619 only (n = 6)	−8.21	0.14	
+ AngaD7L1 (10 μM)	−6.38	0.08	<0.0001
After AngaD7L1 washout	−8.10	0.11	=0.54
Serotonin (5-HT) only (n = 7)	−6.99	0.14	
+ AngaD7L3 (1 μM)	−5.57	0.20	<0.0001
After AngaD7L3 washout	−6.87	0.15	=0.57

LogIC$_{50}$ calculated from four parameter logistic regression, fit to vasoconstriction dose-response curves (*p*-value comparing the peptide and washout against initial constriction agonist).

thromboplastin (aPTT) assays. As expected, neither AngaD7L1 nor AngaD7L3 were involved in the extrinsic or intrinsic pathways (Fig. 4, *B* and *C*). AngaD7L2 did not have an observable effect on the PT pathway. However, time to coagulation *via* the aPTT pathway was significantly increased in the presence of AngaD7L2 ($p = 0.0006^{***}$), confirming its role as an anticoagulant and its specific involvement in the intrinsic coagulation pathway.

AngaD7L2 binds coagulation factors XII, XIIa, and XI as determined by surface plasmon resonance

Because AngaD7L2 displays an anticoagulant activity, we carried out a binding experiment with different coagulation factors involved in the activation of the contact system. The surface plasmon resonance (SPR) experiments show that AngaD7L2 binds to human coagulation factors XII (FXII), XIIa (FXIIa), and XI (FXI), but no interaction was detected with other coagulation factors involved in the extrinsic or intrinsic pathways of coagulation (Fig. 5*A*). The binding affinity constant (K$_D$) of AngaD7L2 and FXII, FXIIa, and FXI were also calculated using SPR analysis (Table 3). Typical sensograms of kinetic experiments are shown in Figure 5, *B*–*D*. The best fit was attained using a two-state reaction model. Similar to hamadarin (24), AngaD7L2 appears to recognize conformational changes of factors XII, XIIa, and XI induced by Zn^{2+} binding. Using this model, the affinity of AngaD7L2 for FXII, FXIIa, and FXI were 16.4 nM, 5.03 nM, and 8.47 nM, respectively (Table 3). Interestingly, AngaD7L2 binds to FXI
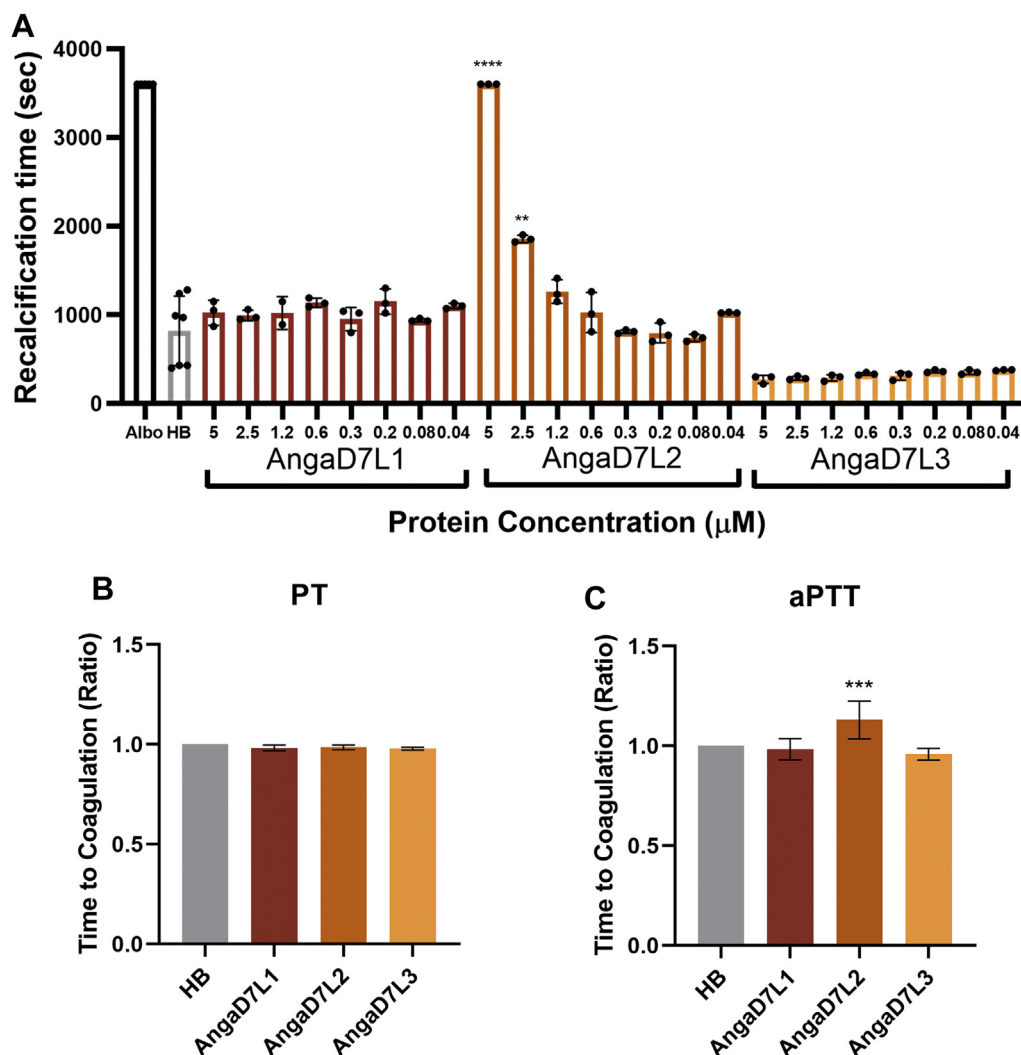
Figure 4. Coagulation assays with AngaD7L1, AngaD7L2, and AngaD7L3 recombinant proteins. *A*, recalcification assays were performed in triplicate with each recombinant protein and time to OD (OD = 0.025) (seconds) was recorded. Alboserpin (3 μM) served as a positive control; Hepes buffer (HB) served as a negative control. Involvement of the AngaD7 long-form proteins in the (*B*) extrinsic and (*C*) intrinsic clotting pathways was tested using PT and aPTT assays. Tests were performed in triplicate. Bars indicate SD. Significance was determined with one-way ANOVA followed by Dunnet's multiple-comparison test using the negative control as the reference ($p < 0.01^{**}$; $p < 0.001^{***}$; $p < 0.0001^{****}$). aPTT, activated partial thromboplastin; PT, prothrombin.

but not FXIa. This effect has also been observed in Beta-Glycoprotein I (β2GPI), a plasma protein with both procoagulant and anticoagulant properties, that binds directly to FXI and prevents generation of FXIa by FXIIa and thrombin *in vitro*. Native and recombinant β2GPI has no influence on the enzymatic activity of FXIa (25).
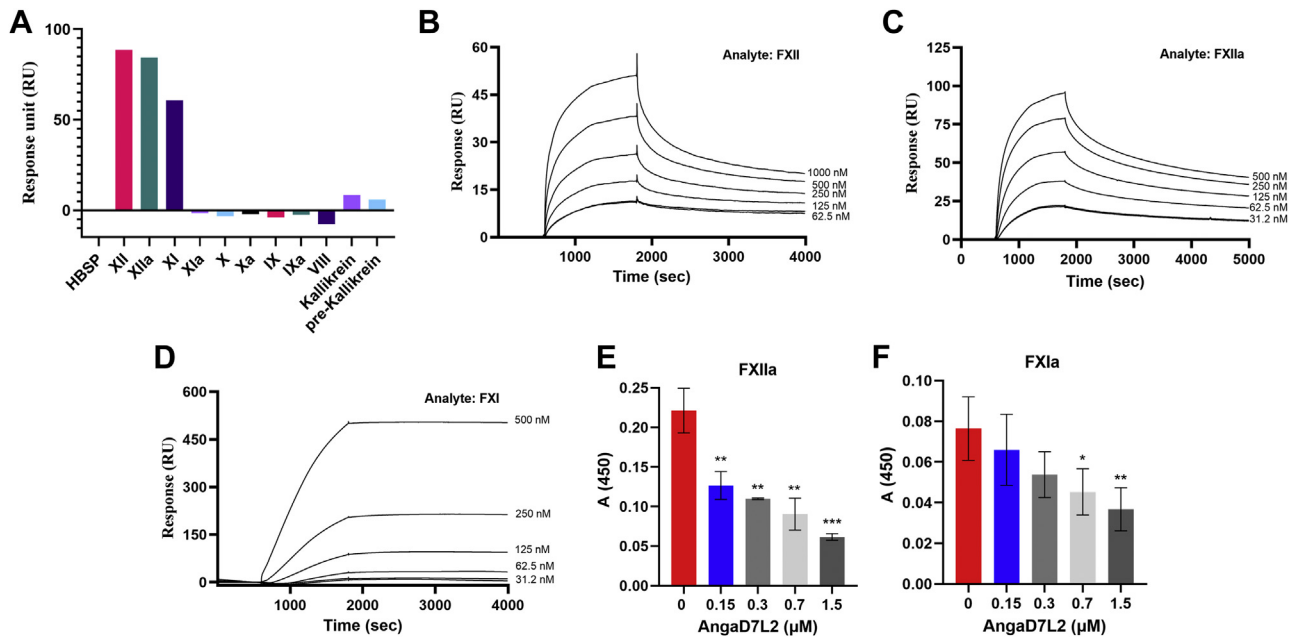
AngaD7L2 inhibits generation of FXIIa and FXIa in normal plasma

We tested whether AngaD7L2 inhibited generation of coagulation factors XIIa and XIa in normal plasma. The contact pathway of coagulation was activated with aPTT reagent in the presence of different concentrations of AngaDL2. The inhibitory activity of AngaD7L2 was evaluated by measuring the cleavage of the specific chromogenic substrates for FXIIa and FXIa. As shown in Figure 5, *E* and *F*, AngaD7L2 inhibited the generation of FXIIa and FXIa in a dose-dependent manner.

We concluded that AngaD7L2 inhibits coagulation by directly binding to FXII and FXIIa, preventing activation and initiation of the extrinsic pathway of coagulation.

Discussion

It is widely known that salivary proteins suppress host hemostasis and inflammation to facilitate the intake of blood by hematophagous arthropods. Arthropods have developed a diverse group of proteins to achieve this, some with unique and others with redundant functions. As one of the most abundant female mosquito salivary proteins, the D7s play an important role in combating host hemostasis. In this work, we characterized the three *A. gambiae* D7 long-form proteins and found unique properties from each other and from other anopheline D7s. We found that the AngaD7L3 shows a similar binding capacity as described for the short-form AngaD7s. It binds only serotonin and no other biogenic amine or

Figure 5. AngaD7L2 binds coagulation factors FXII, FXIIa, and FXI and prevents generation of FXIIa and FXIa in plasma. *A*, SPR-binding test of AngaD7L2 and different coagulation factors. AngaD7L2 was immobilized on sensor CM5 chip, and factors XII, XIIa, XI, XIa, X, Xa, IX, IXa, VIII, Kallikrein, and prekallikrein at 100 nM were flowed over the immobilized protein. *B*, kinetic analysis of AngaD7 with FXII (*B*), FXIIa (*C*), and FXI (*D*). For all SPR assays, the analytes were flowed over immobilized AngaD7L2 at a flow rate of 40 μl/min using a buffer containing 100 μM ZnCl$_2$ and the sensor chip surface was regenerated by a pulse injection of 25 mm EDTA after each experiment. Inhibition of generation of factor XIIa and XIa by AngaD7L2 in human plasma (*E* and *F*). Various concentrations of AngaD7L2 were incubated with normal human plasma and the contact activation was initiated with diluted aPTT reagent (1:50 in PBS). The amidolytic activities of generated factor XIa and factor XIIa were determined by adding the chromogenic substrates Chromogenix S-2366 or Chromogenix S-2302, respectively. Substrate hydrolysis was measured at 405 nm after 30 min. Bars indicate the SEM. Significance was determined with one-way ANOVA followed by Dunnet's multiple-comparison test using the negative control as the reference. aPTT, activated partial thromboplastin; SPR, surface plasmon resonance.

eicosanoid. This is an unexpected result because this is the first known long-form *Anopheles* D7 protein to bind to a biogenic amine. Additionally, we found that the AngaD7L2 exhibited anticlotting activity, a function never previously reported for a mosquito D7 long-form protein.

Sequence alignments comparing the *A. gambiae* D7 long-forms to other D7 proteins showed that AngaD7L1 and AngaD7L2 amino acid sequences of the entire protein are only partially conserved with *A. stephensi* AnSt-D7L1 amino acid sequence. However, within the binding pocket, known amino acid residues involved in lipid binding are highly conserved in AngaD7L1 and completely conserved in AngaD7L2. The solved crystal structure of the AnSt-D7L1 protein in complex with U-46619 ligand demonstrated that U-46619 is stabilized by hydrogen bonding interactions of the omega-5 hydroxyl group with the phenolic hydroxyl group of Tyr-52 (16). Tyr-52 is also present in the *Aedes albopictus* AlboD7L1 and *Aedes aegypti* AeD7L2; however, it is absent in *Ae. aegypti* AeD7L1, which does not bind U-46619 (14). We also found that the

biogenic amine-binding residues in the C-terminal of AngaD7L3 are completely conserved when aligned with the short-form *A. gambiae* D7s and *Ae. aegypti* AeD7L1, which are proteins known to bind serotonin. AngaD7L3 only possesses three of the 11 lipid-binding residues in the N-terminal domain which explains its inability to bind CysLTs and U-46619.

The D7 family of proteins act by scavenging small-molecule effectors of hemostasis and inflammation by having high-affinity ligand-binding sites (3, 5, 6). In this study, we tested several mediators of host hemostasis previously found to bind D7L proteins from other mosquito species and found that AngaD7L1 is capable of binding both leukotriene C$_4$ and the thromboxane A2 (TxA2) analog, U-46619. This is similar to long-form D7 proteins from other mosquito species such as the AnSt-D7L1, *Ae. albopictus* AlboD7L1, *Ae. aegypti* AeD7L2, and *Culex quinquefasciatus* CxD7L2 (Fig. S6) (3, 14, 16, 22, 26–28). *Ae. aegypti* AeD7L1 binds LTC$_4$ but not U-46619. Interestingly, AngaD7L1 did not bind any other leukotriene, unlike the D7s from other mosquito species. Leukotrienes induce inflammatory responses such as pain, swelling, itching, and erythema in the host (4, 29). Thromboxane A2 induces the hemostasis responses of vasoconstriction and platelet aggregation that reduce blood flow to the injury site. AngaD7L2 showed only a weak binding affinity to the leukotrienes LTB$_4$ and LTD$_4$, suggesting that it may be involved in anti-inflammatory activity, however the extent to which it can do so *in vivo* remains to be elucidated. AngaD7L3 did not bind

Table 3
Kinetics of AngaD7L2 and coagulation factors XI, XII, and XIIa in human plasma

Analyte	ka ± SD (1/Ms)	kd ± SD (1/s)	K_D ± SD (nM)
FXI	$9.92 \times 10^4 \pm 3.70 \times 10^4$	$6.96 \times 10^{-3} \pm 1.20 \times 10^{-3}$	8.47 ± 1.15
FXII	$1.25 \times 10^5 \pm 2.83 \times 10^3$	$1.69 \times 10^{-2} \pm 3.05 \times 10^{-3}$	16.4 ± 2.97
FXIIa	$2.03 \times 10^8 \pm 2.86 \times 10^7$	$4.03 \times 10^{-1} \pm 5.48 \times 10^{-1}$	5.03 ± 4.34

A minimum of three replicates were performed for each factor.

any eicosanoids, but it did bind tightly the biogenic amine serotonin. Serotonin induces several hemostatic responses in the host such as vasoconstriction, platelet aggregation, and blood clotting. While most African species of *Anopheles*, for which an annotated genome exists, have three D7 long-form proteins, *Anopheles* from Asia, Pacific, and Americas have only two long-form D7 (17, 30–32). Asian and Pacific *Anopheles* have one (or an incomplete/low quality) D7L1/D7L2 and one D7L3 ortholog, whereas *Anopheles* from the Americas have a D7L1 and D7L2, but no D7L3 ortholog (31). *Anopheles funestus* and *Anopheles christyi* seem to be the only African exceptions possessing fewer than three long-form D7s. *A. funestus* has a D7L3 ortholog and an incomplete/low quality of D7L1/D7L2, whereas *A. christyi* has only a single D7L3 ortholog (31). The short-form *A. gambiae* D7s have a negatively charged patch that biogenic amines bind to that is completely conserved in AngaD7L3 (3). The binding affinity and sequence alignment results indicate that *A. gambiae* D7L3 is behaving similarly to the short-form AngaD7s D7r1-D7r4 (3). Characterizing other African *Anopheles* D7 long-form proteins to see if this is a common trend among mosquitoes possessing three long-form D7s would be interesting to investigate in future studies.

Vasoconstriction, where the blood vessels constrict to prevent further blood loss, is the first step in hemostasis and occurs almost immediately upon tissue injury. AngaD7L1 inhibited vasoconstriction induced by U-46619, while AngaD7L3 inhibited serotonin-induced vasoconstriction. TxA2 is a product of the arachidonic acid metabolism cyclooxygenase pathway (33). TxA2 is released from platelets and smooth muscle during inflammation and injury and is a powerful vasoconstrictor (33, 34). AngaD7L1 has a moderate binding affinity for the TxA2 analog, U-46619, which is why a higher concentration of protein was needed to sequester the U-46619 and significantly reduce the vasoconstrictive effect on the artery. This function is similar to that of D7s from other mosquito species. AnSt-D7L1, AlboD7L1, CxD7L2, and AeD7L2 also bind U-46619 (16, 22, 27, 28). Both AeD7L2 and AnSt-D7L1 were also shown to inhibit vascular contraction (16, 27). Serotonin is a complex substance that can be vasoactive and cause both vasoconstriction and vasodilation (35) and is a vasoconstrictive agonist of mesenteric arteries (36). Since an insect bite injury occurs at the venule level, where serotonin acts mainly as a vasoconstrictor, it often functions as such during hemostasis. When induced by serotonin, AngaD7L3 had a strong vasoconstriction inhibition effect, which further validates its strong binding affinity for serotonin. Based on our results in *ex vivo*–isolated small resistance arteries, it is likely that in *in vivo*, both AngaD7L1 and AngaD7L3 act to prevent vasoconstriction of host blood vessels to aid maintenance of blood flow for feeding.

The second step in hemostasis is platelet aggregation, where platelets stick together to form a temporary plug over the vessel injury. Thromboxane A2 (TxA2) and serotonin, in addition to being vasoconstrictors, are also agonists of platelet aggregation. Both AngaD7L1 and AngaD7L3 had a dose-dependent effect on platelet aggregation when induced by

the stable analog of TxA2, U-46619, or serotonin, respectively. Platelets play an important role in controlling bleeding at the site of blood vessel injury. Activated platelets release TxA2, which is a potent agonist of platelet aggregation. The inhibition of platelet aggregation induced by U-46619 has been reported in other mosquito D7 proteins. AlboD7L1 and CxD7L2 had a low U-46619–induced platelet inhibiting effect because of their low binding affinity to U-46619 (22, 28). AnSt-D7L1 and AeD7L2, which both tightly bind U-46619, displayed a strong inhibition effect on platelet aggregation (16, 27). Alone, serotonin is a weak agonist to platelet aggregation, but it can reduce the threshold concentration of other agonists, such as collagen. By sequestering serotonin, AngaD7L3 prevents the potentiating effect of serotonin on platelet aggregation. This effect has been observed in other non-anopheline mosquito species such as *Ae. albopictus* AlboD7L1 and *C. quinquefasciatus* CxD7L2 (22, 28). The *A. gambiae* short-forms D7r1-D7r4 are also known to bind serotonin and likely inhibit platelet aggregation and vasoconstriction (3).

The third and last step in hemostasis is blood clotting, where coagulated blood reinforces the platelet plug to seal the wound. Blood clotting can be activated by the intrinsic and extrinsic pathways, both converging to the activation of factor X (FX) to FXa, which converts PT to thrombin (37). Many arthropod coagulation inhibitors have been reported (38–40). In mosquitoes, proteins in the serpin family have been associated with factor Xa inhibition. Stark and Jones identified the first salivary serpin with anticlotting activity in *Ae. aegypti* (41, 42). In *Ae. albopictus*, factor Xa inhibition is performed by Alboserpin, a 45-kDa protein belonging to the serpin family of protease inhibitors (23). The short-form *A. gambiae* D7r1 also has anticlotting activity by inhibiting the aPTT time pathway (3). AngaD7L2 is the first D7 long-form protein observed to inhibit blood clotting. AngaD7L2 does this specifically by binding to the factor XII of the intrinsic coagulation pathway. Factor XII plays a role in the activation of classical complement pathway, the fibrinolytic system, and the initiation of cell-mediated inflammatory responses (43). In addition to the anticoagulant activity displayed by AngaD7L2, targeting FXII may prevent the proinflammatory bradykinin-mediated responses *in vivo*, reducing local pain and vasoconstriction and likely helping a successful blood meal intake. Therefore, inflammation induced by bradykinin at the injured site will prove a serious threat for blood-feeding animals. The possible relevance of FXII contact activation in blood feeding *in vivo* is poorly understood and more investigation is needed.

Hematophagous arthropods have diverse salivary molecules that help them evade host hemostasis and successfully take a blood meal. These salivary compounds have evolved independently in different insect families, so that each one has its own unique cocktail of pharmacologically active proteins. In this study, we report two novel Anopheline D7 long-form functions. AngaD7L3 binds the single biogenic amine serotonin, a function previously reported only for short-form *Anopheles* D7s. It would be worth investigating other *Anopheles* D7s to determine if this function is shared among similar species or if this is common in *Anopheles* as it is in among

other mosquito genera. AngaD7L2 anticoagulation is also a unique function for D7 long forms not yet reported in any other mosquito species. These results highlight the complexity of hematophagous arthropod salivary proteins and is likely a function of the continuous evolutionary arms race between arthropods and their hosts.

Experimental procedures

Sequence alignments

Amino acid sequences of the *A. gambiae* long- and short-form D7s, *Ae. aegypti* AeD7L1, *Ae. albopictus* AlboD7L1, *A. stephensi* AnSt-D7L1, and *C. quinquefasciatus* D7L1, and *C. quinquefasciatus* CxD7L1 were retrieved from the Vector-Base database (AGAP008278; AGAP008279; AGAP028120; AGAP008284; AGAP008282; AGAP008283; AGAP008281; AGAP008280; AAEL026087; AALF024477; ASTEI02998; CPIJ014549). Multiple alignments were obtained by Clustal Omega and converted to text files for figure annotation.

Cloning, expression, and purification of A. gambiae long-form proteins

One Shot TOP10 chemically competent *Escherichia coli* (Invitrogen) were transformed with VR2001-TOPO vectors containing the AngaD7L1, AngaD7L2, and AngaD7L3 sequences followed by a 6xHis-tag and a kanamycin resistance gene. Plasmids were isolated and purified from kanamycin-treated bacterial cultures using Nucleobond PC 10000 EF Megaprep kit (Macherey-Nagel). Human embryonic kidney 293F cells were transfected with the respective plasmids at the Frederick National Laboratory for Cancer Research, and supernatants were collected 72 h after transfection. Recombinant proteins were purified by affinity chromatography using Nickel-charged HiTrap Chelating HP columns (Cytiva) followed by size-exclusion chromatography in a HiLoad 16/600 Superdex 200 pg column for AngaD7L1 and AngaD7L3 and in a Superdex 200 Increase 13/300 GL (GE Healthcare) for AngaD7L2 due to small protein amount. Fractions were visualized in Coomassie-stained gels.

Isothermal titration calorimetry

Binding experiments were performed using a MicroCal PEAQ-ITC (Malvern Panalytical). AngaD7L1, AngaD7L2, and AngaD7L3 recombinant proteins were diluted to 5 μM in TBS (20 mM Tris–HCl, 150 mM NaCl, pH 7.4) and ligands (leukotrienes B_4, C_4, D_4, and E_4, U-46619, serotonin, histamine, epinephrine, norepinephrine, and tryptamine) were diluted to 50 μM in TBS. For lipid ligands (leukotrienes and U-46619), the solvent was evaporated under a stream of nitrogen gas and resuspended in TBS, vortexed, and sonicated for 10 min. Protein and ligand samples were degassed using a MicroCal ThermoVac (Malvern Panalytical) prior to loading. Injections of 10 μl ligand were added to 200 μl of protein every 150 s. Assays were performed at 30 °C and spun at 750 rpm. Stoichiometries indicated a single binding site for each ligand and therefore binding affinities were calculated using a single ligand-binding model (N = 1).

The calorimetric enthalpy (ΔH^{cal}) for each injection was calculated, and binding isotherms were fitted according to a model for a single binding site by nonlinear squares analysis using Microcal Origin software. The enthalpy change (ΔH) and stoichiometry (n) were determined using (Equation 1),

$$Q = n\Phi Mt\Delta HV_o \qquad (1)$$

where Q is the total heat content of the solution contained in the cell volume (V_o) at fractional saturation Φ, ΔH is the molar heat of ligand binding, n is the number of sites, and Mt is the bulk concentration of macromolecule in V_o.

The nM range of K_D values from tight binding protein–ligand interactions is challenging to get in ITC instruments because of the narrow window between getting enough data points and getting a high enough heat change detectable by the instrument. This problem is exacerbated with the PEAQ ITC instrument because of the small cell volume capacity and limitation is sensitivity of the instrument, leading to a large viability and standard deviation between runs.

Platelet aggregation assays

Platelet-rich plasma was obtained from normal healthy donors on the NCI IRB-approved NIH protocol 99-CC-0168, 'Collection and Distribution of Blood Components from Healthy Donors for *In Vitro* Research Use'. Blood donors provide written informed consent, and platelets were de-identified prior to distribution. Human platelet-rich plasma (∼250,000 platelets/μl final density) and Tyrode–bovine serum albumin buffer in the presence or absence of AngaD7L1, AngaD7L2, or AngaD7L3 recombinant protein (0.3 μM, 1 μM, or 3 μM) were placed in a Chrono-Log aggregometer model 700 (Chrono-Log Corporation) and stirred at 1200 rpm at 37 °C for 1 min prior to the addition of different agonists (0.3 or 0.7 μM U-46619; 0.8 μM serotonin).

Vasoconstriction/myography assay

Euthanasia and collection of murine mesenteric arteries

Public Health Service Animal Welfare Assurance #A4149-01 guidelines were followed according to the National Institute of Allergy and Infectious Diseases (NIAID), National Institutes of Health (NIH) Animal Office of Animal Care and Use (OACU). These studies were carried out according to the NIAID-NIH animal study protocol (ASP) approved by the NIH Office of Animal Care and Use Committee, with approvals ID ASP-LMVR-3 and ASP-LMVR-21E. While deeply anesthetized by inhalational isoflurane (furane 4%), each mouse was euthanized by bilateral pneumothorectomy, after which the small intestine was removed from the abdomen and placed in cold modified Krebs–Hepes buffer (KH buffer, pH 7.4; 4 °C). The KH buffer had the following composition 130 mM NaCl, 4.7 mM KCl, 1.20 mM KH_2PO_4, 1.20 mM $MgSO_4$ - $7H_2O$, 14.9 mM $NaHCO_3$, 11 mM Dextrose, 1.6 mM $CaCl_2$, and 10 mM Hepes. Third-order arteries were dissected from the mesentery of the small intestine and placed into an isolated microvessel chamber (Danish Myo Technologies)

filled with KH buffer at 37 °C. Each mesenteric artery was subsequently doubly cannulated within this heated chamber (37 °C) to allow the lumen and exterior of the vessel to be perfused and superfused, respectively, with KH buffer from separate reservoirs. The perfusing buffer reservoir was pressurized with room air.

Measurements of vascular reactivity in isolated mesenteric arteries by pressure myography

The heated microvessel chambers described above were placed on a 10× video microscope (Danish Myo Technologies). Each mesenteric artery was allowed to equilibrate for 60 min at a pressure of 60 mmHg to approximate *in vivo* perfusion pressure of third-order murine mesenteric arteries. Any vessel that did not demonstrate significant vasoconstriction to 10 μM KCl at the equilibration pressure was discarded. Following equilibration, the vasoconstrictor reactivity of each artery was assessed in response to escalating logarithmic doses of the vasoconstrictive agonists U-46619 or serotonin (5-HT). The applied concentrations of the vasoconstrictive agonists were U-46610 (10^{-9} M–10^{-4} M) and 5-HT (10^{-9} M–10^{-4} M). Vessel diameter was measured by digital caliper micrometer measurement of the video microscope using DMT MyoVIEW software (Danish Myo Technologies). Vessel diameter was measured continuously prior to agonist application and following each application of agonist from 10^{-9} M to 10^{-4} M. The vascular response to U-46619 or 5-HT was calculated as the percentage constriction from baseline: the change in diameter between the maximum constricted diameter at each dosage of agonist was plotted as percentage change in diameter compared to the vessel resting baseline diameter. Following completion of the dose-response curve, vessels within the myograph chambers were washed 3× with KH buffer and allowed to equilibrate to baseline diameter.

The constriction response measurements to U-46619 or 5-HT were then repeated in the presence of arteries incubated with salivary gland protein AngaD7L1 (10 μM, applied in arteries constricted with U-46619) or AngaD7L3 (1 μM, applied in arteries constricted with 5-HT). Following completion of the dose-response curve in presence of the salivary gland proteins, vessels within the myograph chambers were again washed 3× with KH buffer and allowed to equilibrate to baseline diameter. A final constriction response curve was performed after salivary protein washout. Two-third order mesenteric arteries were taken from a total of seven mice (four male, three female). From each mouse, one artery was constricted first with U-46619, then with U-46619 in the presence of AngaD7L1 (10 μM), and lastly with U-46619 following washout of AngaD7L1. The second artery was constricted first with 5-HT, then with 5-HT in the presence of AngaD7L3 (1 μM), and lastly with 5-HT following washout of AngaD7L3. For each artery, two measurements of the inner arterial diameter were averaged for each dosage of vasoconstrictive agonist. A total of n = 7 arteries were measured for response to serotonin, and n = 6 (three male, three female) arteries were used for constriction with U-46619 due to functional loss of an artery during experimental preparation.

For each treatment condition, the dose-response curve to the vasoconstrictive agonist was fit with a four-parameter logistic regression, from which the logIC50—the concentration of constrictive agonist at which 50% of the total constriction was achieved—was calculated. The logIC50 for the initial constrictive response was compared with the logIC50 following incubation with either AngaD7L1 or AngaD7L3 protein to determine whether the proteins had significantly increased the logIC50. The logIC50 of the washout curve was compared to the initial response to test whether incubation with the proteins had fundamentally altered arterial reactivity. LogIC50 values and their SEM were compared statistically by Welch's *t* test (GraphPad Prism v9.0.0).

Plasma recalcification assay

To measure recalcification time of human plasma, 30 μl of BIOPHEN normal control plasma (Hyphen BioMed) was mixed with equal volumes of serially diluted recombinant protein samples (15 μM–0.1 μM), Hepes buffer (10 mM Hepes, 150 mM NaCl, pH 7.3) (negative control), or 3 μM Alboserpin (positive control) [23] in a 96-well flat-bottom plate and incubated for 2 min at 37 °C. The coagulation cascade was triggered by adding 30 μl of prewarmed 25 mM $CaCl_2$ to each well. Data was collected in a VersaMax plate reader (Molecular Devices) at 10-s intervals over 60 min. Recalcification was determined as the time for each sample to reach 0.025 absorption units at 650 nm.

Tests of intrinsic and extrinsic clotting pathways

AngaD7L2 was subjected to PT time and aPTT time tests using a Start4 Hemostasis Analyzer (Diagnostica Stago). BIOPHEN normal control plasma (50 μl) (Hyphen BioMed) was incubated with 5 μl of either Hepes buffer (negative control), Alboserpin (3 μM) (positive control) [23], or recombinant protein diluted in Hepes buffer (15 μM), and incubated at 37 °C for 2 min. For PT, 100 μl of Neoplastine CI Plus reagent (Diagnostica Stago) was added and the clotting time was recorded under stirring conditions. For aPTT, 50 μl of aPTT reagent was added to the mixture of protein and plasma and incubated for 3 min at 37 °C. Clotting was triggered by the addition of 50 μl of prewarmed 25 mM $CaCl_2$. Time to clotting was recorded and the results were converted to ratios and analyzed for significance using pairwise t-tests (p = 0.05).

SPR analysis

All SPR experiments were carried out in a T200 instrument (GE Healthcare) following the manufacturer's instructions. Sensor CM5, amine coupling reagents, and buffers were purchased from Cytiva Life Sciences. Running buffer HBS-P (10 mM Hepes, pH 7.4, 150 mM NaCl, and 0.005% (v/v) surfactant P20) supplemented with 100 μM $ZnCl_2$ was used for all SPR experiments. The Biacore T200 Evaluation software v3.2 was used for kinetic evaluations, and the data fitted using

the two-state binding model (conformational change). AngaD7L2 (30 mg/ml) in 10 mM acetate buffer, pH 4.5 was immobilized on a CM5 sensor *via* amine coupling. A blank flow cell, without ligand, was used to subtract the buffer effect. Binding experiments were carried out with a contact time of 120 s at a flow rate of 40 μl/min at 25 °C and the complex dissociation monitored for 120 s. The sensor surface was regenerated by a pulse injection of 25 mM EDTA after each cycle. Human coagulation factors were at 100 nM concentration in running buffer. For kinetic experiments, FXII, FXIIa, and FXI were flowed over immobilized AngaD7L2 at 40 ml/min. Complex dissociation was monitored for 2000 s, and the sensor surface regenerated by a pulse of 20 s of 25 Mm EDTA at 40 μl/min. Binding and kinetic analysis were carried out in duplicate.

Generation of FXIIa and FXIa in normal plasma

To assess the inhibitory effects of AngaD7L2 on the extrinsic pathway of coagulation, we monitored the generation of activated contact factors XIIa and XIa *in vitro*. Human reference plasma (30 μl) (Diagnostica Stago) was preincubated with AngaD7L2 (30 μl) at different concentrations. After 10 min at room temperature, 30 μl of diluted (1:50 in PBS) aPTT reagent (Helena Laboratories) was added to activate the contact system. After 10 min, the chromogenic substrate from Chromogenix S2302 (FXIIa) or S2366 (FXIa) were added to a final concentration of 0.2 mM, and the amidolytic activity of the generated factors was monitored at 405 nm for 30 min using a VersaMax microplate reader (Molecular Devices). All experiments were carried in duplicate.

Data availability

All representative data are contained within the article.

References

1. WHO (2019) *World Malaria Report*, World Health Organization, Geneva
2. Ribeiro, J. M. C. (1995) Blood-feeding arthropods: Live syringes or invertebrate pharmacologists? *Infect. Agents Dis.* **4**, 143–152
3. Calvo, E., Mans, B. J., Andersen, J. F., and Ribeiro, J. M. C. (2006) Function and evolution of a mosquito salivary protein family. *J. Biol. Chem.* **281**, 1935–1942
4. Boyce, J. A. (2007) Mast cells and eicosanoid mediators: A system of reciprocal paracrine and autocrine regulation. *Immunol. Rev.* **217**, 168–185
5. Andersen, J. F., Francischetti, I. M., Valenzuela, J. G., Schuck, P., and Ribeiro, J. M. (2003) Inhibition of hemostasis by a high affinity biogenic amine-binding protein from the saliva of a blood- feeding insect. *J. Biol. Chem.* **278**, 4611–4617
6. Mans, B. J., Ribeiro, J. M., and Andersen, J. F. (2008) Structure, function and evolution of biogenic amine-binding proteins in soft ticks. *J. Biol. Chem.* **283**, 18721–18733
7. James, A. A., Blackmer, K., Marinotti, O., Ghosn, C. R., and Racioppi, J. V. (1991) Isolation and characterization of the gene expressing the major salivary gland protein of the female mosquito, Aedes aegypti. *Mol. Biochem. Parasitol.* **44**, 245–253
8. Mans, B. J., Calvo, E., Ribeiro, J. M., and Andersen, J. F. (2007) The crystal structure of D7r4, a salivary biogenic amine-binding protein from the malaria mosquito Anopheles gambiae. *J. Biol. Chem.* **282**, 36626–36633
9. Ribeiro, J. M., and Arca, B. (2009) From sialomes to the sialoverse: An insight into salivary potion of blood-feeding insects. *Adv. Insect Physiol.* **37**, 59–118
10. Lanfrancotti, A., Lombardo, F., Santolamazza, F., Veneri, M., Castrignanò, T., Coluzzi, M., and Arcà, B. (2002) Novel cDNAs encoding salivary proteins from the malaria vector Anopheles gambiae. *FEBS Lett.* **517**, 67–71
11. Arcà, B., Lombardo, F., de Lara Capurro, M., della Torre, A., Dimopoulos, G., James, A. A., and Coluzzi, M. (1999) Trapping cDNAs encoding secreted proteins from the salivary glands of the malaria vector Anopheles gambiae. *Proc. Natl. Acad. Sci. U. S. A.* **96**, 1516–1521
12. Arcà, B., Lombardo, F., Lanfrancotti, A., Spanos, L., Veneri, M., Louis, C., and Coluzzi, M. (2002) A cluster of four D7-related genes is expressed in the salivary glands of the African malaria vector Anopheles gambiae. *Insect Mol. Biol.* **11**, 47–55
13. Arcà, B., Lombardo, F., Valenzuela, J. G., Francischetti, I. M. B., Marinotti, O., Coluzzi, M., and Ribeiro, J. M. C. (2005) An updated catalogue of salivary gland transcripts in the adult female mosquito, Anopheles gambiae. *J. Exp. Biol.* **208**, 3971–3986
14. Calvo, E., Mans, B. J., Ribeiro, J. M., and Andersen, J. F. (2009) Multifunctionality and mechanism of ligand binding in a mosquito antiinflammatory protein. *Proc. Natl. Acad. Sci. U. S. A.* **106**, 3728–3733
15. Suwan, N., Wilkinson, M. C., Crampton, J. M., and Bates, P. A. (2002) Expression of D7 and D7-related proteins in the salivary glands of the human malaria mosquito Anopheles stephensi. *Insect Mol. Biol.* **11**, 223–232
16. Alvarenga, P. H., Francischetti, I. M., Calvo, E., Sa-Nunes, A., Ribeiro, J. M., and Andersen, J. F. (2010) The function and three-dimensional structure of a thromboxane A2/cysteinyl leukotriene-binding protein from the saliva of a mosquito vector of the malaria parasite. *PLoS Biol.* **8**, e1000547
17. Calvo, E., Pham, V. M., Marinotti, O., Andersen, J. F., and Ribeiro, J. M. (2009) The salivary gland transcriptome of the neotropical malaria vector Anopheles darlingi reveals accelerated evolution of genes relevant to hematophagy. *BMC Genomics* **10**, 57
18. Valenzuela, J., Charlab, R., Gonzalez, E., Miranda-Santos, I., Marinotti, O., Francischetti, I., and Ribeiro, J. (2002) The D7 family of salivary proteins in blood sucking diptera. *Insect Mol. Biol.* **11**, 149–155

19. Sahid, M., Tripathi, T., Sobia, F., Moin, S., Siddiqui, M., and Khan, R. (2009) Histamine, histamine receptors, and their role in immunomodulation: An updated systematic review. *Open Immunol. J.* **2**, 9–41

20. Andrews, R. K., and Berndt, M. C. (2004) Platelet physiology and thrombosis. *Thromb. Res.* **114**, 447–453

21. Brass, L. (2010) Understanding and evaluating platelet function. *Hematol. Am. Soc. Hematol. Educ. Program* **2010**, 387–396

22. Martin-Martin, I., Smith, L., Chagas, A., Sá-Nunes, A., Shrivastava, G., Valenzuela-Leon, P., and Calvo, E. (2020) Aedes albopictus D7 salivary protein prevents host hemostasis and inflammation. *Biomolecules* **10**, 1372

23. Calvo, E., Mizurini, D., Sá-Nunes, A., Ribeiro, J., Andersen, J., Mans, B., Monteiro, R., Kotsyfakis, M., and Francischetti, I. (2011) Alboserpin, a factor Xa inhibitor from the mosquito vector of yellow fever, binds heparin and membrane phospholipids and exhibits antithrombotic activity. *J. Biol. Chem.* **286**, 27998–28010

24. Isawa, H., Yuda, M., Orito, Y., and Chinzei, Y. (2002) A mosquito salivary protein inhibits activation of the plasma contact system by binding to factor XII and high molecular weight kininogen. *J. Biol. Chem.* **277**, 27651–27658

25. Shi, T., Iverson, G. M., Qi, J. C., Cockerill, K. A., Linnik, M. D., Konecny, P., and Krilis, S. A. (2004) β2-glycoprotein I binds factor XI and inhibits its activation by thrombin and factor XIIa: Loss of inhibition by clipped β2-glycoprotein I. *Proc. Natl. Acad. Sci. U. S. A.* **101**, 3939–3944

26. dos Santos Malafronte, R., Calvo, E., James, A., and Marinotti, O. (2003) The major salivary gland antigens of Culex quinquefasciatus are D7-related proteins. *Insect Biochem. Mol. Biol.* **33**, 63–71

27. Martin-Martin, I., Kern, O., Brooks, S., Smith, L. B., Valenzuela-Leon, P. C., Bonilla, B., Ackerman, H., and Calvo, E. (2020) Biochemical characterization of AeD7L2 and its physiological relevance in blood feeding in the dengue mosquito vector, Aedes aegypti. *FEBS J.* **288**, 2014–2029

28. Martin-Martin, I., Paige, A., Valenzuela, P., Gittis, A., Kern, O., Bonilla, B., Campos Chagas, A., Ganesan, S., Smith, L., Garboczi, D., and Calvo, E. (2020) ADP binding by the Culex quinquefasciatus mosquito D7 salivary protein enhances blood feeding on mammals. *Nat. Commun.* **11**, 2911

29. Soter, N. A., Lewis, R. A., Corey, E. J., and Austen, K. F. (1983) Local effects of synthetic leukotrienes (LTC4, LTD4, LTE4, and LTB4) in human skin. *J. Invest. Dermatol.* **80**, 115–119

30. Calvo, E., Andersen, J., Francischetti, I. M., deL Capurro, M., deBianchi, A. G., James, A. A., Ribeiro, J. M. C., and Marinotti, O. (2004) The transcriptome of adult female Anopheles darlingi salivary glands. *Insect Mol. Biol.* **13**, 73–88

31. Neafsey, D. E., Waterhouse, R. M., Abai, M. R., Aganezov, S. S., Alekseyev, M. A., Allen, J. E., Amon, J., Arcà, B., Arensburger, P., Artemov, G., Assour, L. A., Basseri, H., Berlin, A., Birren, B. W., Blandin, S. A., *et al.* (2015) Mosquito genomics. Highly evolvable malaria vectors: The genomes of 16 Anopheles mosquitoes. *Science* **347**, 1258522

32. Scarpassa, V. M., Debat, H. J., Alencar, R. B., Saraiva, J. F., Calvo, E., Arcà, B., and Ribeiro, J. M. C. (2019) An insight into the sialotranscriptome and virome of Amazonian anophelines. *BMC Genomics* **20**, 166

33. Narumiya, S., Sugimoto, Y., and Ushikubi, F. (1999) Prostanoid receptors: Structures, properties, and functions. *Physiol. Rev.* **79**, 1193–1226

34. Bolla, M., You, D., Loufrani, L., Levy, B. I., Levy-Toledano, S., Habib, A., and Henrion, D. (2004) Cyclooxygenase involvement in thromboxane-dependent contraction in rat mesenteric resistance arteries. *Hypertension* **43**, 1264–1269

35. Vanhoutte, P. M., and Houston, D. S. (1986) Serotonin, platelets, and vascular function. In: Magro, A., Osswald, W., Reis, D., Vanhoutte, P., eds. *Central and Peripheral Mechanisms of Cardiovascular Regulation*, NATO ASI Series Ed, Springer, Boston, MA: 135–161

36. Wolf, K., Braun, A., Haining, E. J., Tseng, Y.-L., Kraft, P., Schuhmann, M. K., Gotru, S. K., Chen, W., Hermanns, H. M., Stoll, G., Lesch, K.-P., and Nieswandt, B. (2016) Partially defective store operated calcium entry and hem (ITAM) signaling in platelets of serotonin transporter deficient mice. *PLoS One* **11**, e0147664

37. Monroe, D. M., Hoffman, M., and Roberts, H. R. (2002) Platelets and thrombin generation. *Arterioscler. Thromb. Vasc. Biol.* **22**, 1381–1389

38. Francischetti, I. M., Valenzuela, J. G., and Ribeiro, J. M. (1999) Anophelin: Kinetics and mechanism of thrombin inhibition. *Biochemistry* **38**, 16678–16685

39. Koh, C. Y., and Kini, R. M. (2009) Molecular diversity of anticoagulants from haematophagous animals. *Thromb. Haemost.* **102**, 437–453

40. Valenzuela, J. G., Charlab, R., Mather, T. N., and Ribeiro, J. M. (2000) Purification, cloning, and expression of a novel salivary anticomplement protein from the tick, Ixodes scapularis. *J. Biol. Chem.* **275**, 18717–18723

41. Stark, K. R., and James, A. A. (1995) A factor Xa-directed anticoagulant from the salivary glands of the yellow fever mosquito Aedes aegypti. *Exp. Parasitol.* **81**, 321–331

42. Stark, K. R., and James, A. A. (1998) Isolation and characterization of the gene encoding a novel factor Xa-directed anticoagulant from the yellow fever mosquito, Aedes aegypti. *J. Biol. Chem.* **273**, 20802–20809

43. Røjkjær, R., and Schousboe, I. (1997) Partial identification of the Zn2+-binding sites in factor XII and its activation derivatives. *Eur. J. Biochem.* **247**, 491–496